

“Va-et-Vient” spectroscopy: a new mode for faint object CCD spectroscopy with very large telescopes*

J.C. Cuillandre¹, B. Fort¹, J.P. Picat², G. Soucail¹, B. Altieri³, F. Beigbeder², J.P. Dupin¹, T. Pourthié¹, G. Ratier⁴

¹ Laboratoire d’Astrophysique de Toulouse URA-CNRS 285, Observatoire Midi-Pyrénées, UPS, 14 Avenue E. Belin, F-31400 Toulouse, France

² Observatoire du Pic-du-Midi URA-CNRS 1281, Observatoire Midi-Pyrénées, UPS, 9 Rue du Pont de la Moulette, F-65200 Bagnères-de-Bigorre, France

³ Astrophysics Division, European Space Agency, P.O. Box 299, 2200 AG, Noordwijk, The Netherlands

⁴ European Southern Observatory, Karl Schwarzschild Strasse 2, D-8046 Garching bei Munchen, Germany

Submitted May 1, 1993; accepted July, 1993

Abstract. After a review of the sources of noise in faint object low resolution spectroscopy, we discuss the limitations in the S/N ratio due to the flat-fielding errors and sky line sampling residuals after sky subtraction. These errors become rapidly dominant with high flux, and limit the S/N at very low resolution. In order to partly cancel these difficulties, we propose a new observing mode for faint object spectroscopy, called “Va-et-Vient” spectroscopy. Thanks to multiple back-and-forth shifts of charges on the CCD, synchronized with the telescope shifts, the object and a close reference sky are integrated in the same physical conditions on the CCD through the spectrograph. This method enables us to stay in a photon noise regime on long sky background noise limited exposures. A laboratory experiment has been developed to test the feasibility of the method and has been fully exploited. The results are presented in the paper, as well as some preliminary comments on tests obtained on the ESO NTT to evaluate the merit of this approach for the next generation of very large telescopes. A gain of one to two magnitudes, compared with limited actual performances, should be achieved with the new generation of very large telescopes.

Key words: Instrumentation: detectors – data analysis – Methods: observations – Techniques: spectroscopic

1. Introduction

Over the last five years, faint object spectroscopy with long slits has become a necessity in extragalactic astronomy, as people are interested in observing fainter and fainter objects for measuring redshifts and velocity dispersions or studying spectral energy distributions. For example, the deep spectroscopic

surveys performed by Colless et al., the so-called LDSS (1990, 1993) or by Lilly et al. (1991) and Cowie et al. (1993) reach B-magnitudes of 23 to 24. In this magnitude range, the brightness of the objects is less than a tenth of the dark sky brightness in the continuum and a few hundredths of the strong sky emission lines. The sky is then the dominant signal in the CCD spectra, and its subtraction becomes the most critical step in the data reduction to preserve the background photon noise limit. If everything was perfect, with negligible CCD readout noise, the signal-to-noise ratio (S/N) of the spectra should grow as the square-root of the flux so that, for a given spatial scale and resolution, any increase of the telescope diameter or the exposure time should allow the observers to get fainter spectra. In practice, on a given instrument, the S/N tends to reach an upper limit when the total exposure time increases. This is due to some sources of noise which are proportional to the signal, such as flat-fielding residuals and spectral lines sampling residuals occurring in the sky subtraction. The smaller the resolution, the faster the limit is reached. As an example, on a 4-meter telescope with a resolution $R = 300$, the typical exposure time to approach the saturation in sky line spectral domains is a few hours. It is worse for very low resolution ($R \simeq 100$ or, equivalently, a dispersion of $20 \text{ \AA}/\text{pixel}$), especially in the red where the strong and complex sky emission lines dominate. It is quite impossible to use such a low resolution spectroscopic mode on faint distant galaxies for a determination of their global spectral energy distribution in the red because the sky residuals are too strong to allow the measurement of the mean flux level of the underlying object. Such a limitation can also be reached for higher spectral resolution although with longer exposure times. With the next generation of very large telescopes such as Keck 10-m Telescope or the ESO 8-meter VLTs, the gain in limiting magnitude expected by the increase of the collecting power will be partly lost if the high photon noise regime cannot be preserved.

To overcome this limitation, we propose a technique so-called “Va-et-Vient” spectroscopy to minimize the multiplicative errors due to the residuals of the spectral line sampling, the flat-fielding and the temporal sky variations. In this mode,

Send offprint requests to: J.C. Cuillandre

* This concept was initially introduced in the IFOS Consortium Proposal for the faint object spectrograph of the ESO-VLT, presented by the Toulouse Observatory, the Trieste Observatory and the Kapteyn Sterrenwacht.

the (Sky+Object) and the (Sky) reference spectra are integrated on the CCD exactly in the same way through the same slit, on the same pixels and in time intervals that are short compared to the characteristic time scale of the sky fluctuations. After a short analysis of the different sources of noise and the S/N for faint object spectroscopy, we discuss some ways to improve the S/N in Section 2 where the “Va-et-Vient” spectroscopy is introduced. We compare the two methods and predict a factor of merit of the “Va-et-Vient” mode with respect to the long slit mode. In Section 3, we describe in more details a laboratory experiment to test the feasibility of the “Va-et-Vient” spectroscopic mode. The data analysis and the quantitative performances of the experiment are presented in Section 4. Preliminary tests were also recently performed at ESO and will be presented in a forthcoming paper when the whole set of tests on a telescope will be completed. They are rapidly mentioned in Section 5, as well as some conclusions about the possible future of the “Va-et-Vient” spectroscopy.

2. Observing modes for faint object spectroscopy

2.1. Noise analysis in the long slit spectroscopic mode

Let us consider a CCD spectroscopic exposure with an integration time T . After the CCD readout, the sky signal in electrons per spectral element and time unit at a given wavelength is noted ϕ_S . After the sky subtraction procedure, the estimate of the object signal can be written as:

$$\Phi_O = \phi_O T + \langle \phi_S - \phi_{S'} \rangle T \quad (1)$$

where the residuals in the sky subtraction ($\langle \phi_S - \phi_{S'} \rangle$) are considered as a component of the signal error. ϕ_O is the object signal per second. For simplicity, we will assume that the object has a uniform brightness through the slit. The object to sky brightness ratio is defined by $\alpha = \phi_O/\phi_S$ and as we are interested in very faint object spectroscopy ($\alpha \ll 1$), the photon noise is dominated by the sky signal. After sky subtraction, the error estimate for a given spectral element can be written in units of electrons as a contribution of quadratic errors or noises (σ) plus systematic multiplicative errors (μ):

$$N = \sqrt{\sigma_{CCD}^2 + \sigma_{photon}^2 + \mu_{sky} + \mu_{flat} + \mu_{lines}} \quad (2)$$

σ_{CCD}^2 is the variance of the CCD readout noise, which is generally negligible for the new generation of CCDs ($\sigma_{CCD} < 10$ electrons). σ_{photon} is the sky background photon noise, and the three other terms are additional residuals due to the spatial sky fluctuations (μ_{sky}), the flat-fielding (μ_{flat}) and the undersampling of the emission lines (μ_{lines}). These multiplicative errors μ will be constant in any successive signal integration, provided we keep a fixed position of the object on the slit. In other words, they are reproducible on a fixed pixel of the CCD.

The photon noise after sky subtraction is expressed as:

$$\sigma_{photon} = \sqrt{\phi_S(1+u)} \sqrt{T} \quad (3)$$

The parameter u can be varied from 1 to 0, depending on the accuracy with which the sky reference is subtracted. With the use of optimum modelling techniques in long slit spectroscopy, u is set to 0.

$\mu_{sky} = \tau \phi_S T$ is the error due to the spatial fluctuations of the sky brightness. The relative spatial variation of the sky

τ is of the order of 1% over a scale of 1 arcminute, if one takes into account the faint galaxy counts at a brightness level of 27 (Tyson 1988). In the following, we will not discuss this parameter as standard methods for sky subtraction are now implemented in most of the data analysis systems (IRAF, MIDAS, etc ...), using a 2D spatial modelling of the sky under the object as proposed by Horne (86) or Robertson (86).

$\mu_{flat} = \epsilon \phi_S(1+u) T$ is the error due to residuals in the flat-field correction after subtraction. If we consider ϵ as a spatially random error over the surface of the CCD, the typical value for a thick CCD without any fringing is less than 1% (Tyson 1986) in spectroscopic mode where the flat-fields are obtained with internal calibration lamps.

$\mu_{lines} = \omega \phi_S T$ is to the first order approximation the noise due to the different sampling of the same sky lines under the object and on the reference sky (caused, for example, by a slit or a grism misalignment), ω is given by:

$$\omega = \frac{\phi_{S(\lambda)} - \phi_{S'(\lambda+md)}}{\phi_{S(\lambda)}} \simeq \frac{m d}{f(\lambda)} \left(\frac{\partial f(\lambda)}{\partial \lambda} \right) \quad (4)$$

where $f(\lambda)$ is the line profile, d is the dispersion in $\text{\AA}/\text{pixel}$ and m is the misalignment of the spectrum between adjacent pixels as a fraction of a pixel. The steeper the profile, the larger the variation of ω is. This is dramatically true for the narrow and strong sky lines which are undersampled at low resolution. As an illustration, with a small slit misalignment of 10^{-3} (1 pixel over 1000), a dispersion of $10 \text{ \AA}/\text{pixel}$, a value $\omega = 0.1$ is obtained as soon as the variation $f(\lambda)$ from a pixel to the adjacent one is 50%, with a distance of 20 pixels between the sky and (sky+object) spectra. In order to reduce ω , an usual way is to use a pixel oversampling of the sky lines and finally numerical binning of the pixels to recover the full S/N . Working this way, Cowie and Lilly (1989) obtained nice results on galaxies as faint as $B \sim 24$ with a good sky subtraction and adding several exposures with the object stepped in different positions along the slit. This second point is a technique similar to the so-called “shift-and-add” technique developed for very deep photometry (Tyson, 1990). If we consider that the flat-field residuals are not spatially correlated on the CCD, one can increase the final S/N on a long equivalent exposure by offsetting the telescope between each of the n exposures in the direction of the slit. This method is not powerful because the relative multiplicative error is expected to vary slowly as $1/\sqrt{n}$ and the exposure time needed for each exposure to be in the photon noise regime is long. Even with a low readout noise CCD (less than 5 electrons), it takes at least 30 minutes to reach this regime on a 4-meter telescope with a dispersion of $10 \text{ \AA}/\text{pixel}$.

2.2. Comments on the Signal-to-Noise ratio in long slit spectroscopy

In long slit spectroscopic mode (LS), a model of the reference sky spectrum is computed over a large number of CCD rows and u is set to 0.

The S/N per spectral element can be expressed in the form:

$$\left(\frac{S}{N} \right)_{LS} = \frac{\phi_O T}{\sqrt{\phi_S T + \sigma_{CCD}^2 + (\epsilon + \omega) \phi_S T}} \quad (5)$$

Table 1. Evaluation of the limiting factors in the S/N for two long slit spectrographs in two sky regimes. For the sky continuum, we used the values $\epsilon = 0.01$ and $\omega = 0$ while for the sky lines, we used $\epsilon = 0.01$ and $\omega = 0.05$. p is the pixel size in arcsec. and $\delta\lambda$ is the resolution slitwidth in \AA . η is the CCD quantum efficiency in electrons per photon. The S/N is evaluated on 1 pixel, although the pixel size differs and the spectra on EMMI are oversampled by a factor of 2. It is also computed for an object-to-sky ratio of 0.1. Note the strong dependence of T_{LS}^{Sat} on the instrumental set up.

	D (Tel) (cm)	p (")	$\delta\lambda$ (1.5 "slit)		η (e ⁻ /photon)	ϕ_S (e ⁻ /s)	T_{LS}^{Sat} (hours)	$(S/N)_{LS}^{lim}$
EFOSC + RCA2	360	0.675	15 \AA	Sky continuum ($\lambda \sim 5500 \text{\AA}$)	0.27	0.28	5	10
				Sky emission lines ($\lambda \sim 8000 \text{\AA}$)	0.10	0.21	0.4	2
EMMI + THX	350	0.44	13 \AA	Sky continuum ($\lambda \sim 5500 \text{\AA}$)	0.12	0.044	28	10
				Sky emission lines ($\lambda \sim 8000 \text{\AA}$)	0.05	0.036	2	2

As $\phi_S T$ increases (smaller resolution, larger exposure time or larger telescope), the S/N saturates to expression:

$$\left(\frac{S}{N}\right)_{LS}^{lim} = \frac{\alpha}{\epsilon + \omega} \quad (6)$$

The effect is faster near the strong emission lines where ω can dominate the flat-field residuals ϵ (see Figures 5 and 6 below). The limiting value in the S/N does not explicitly depend on the exposure time or the size of the telescope but it depends intrinsically on the spectral element. Using a VLT in this “saturated” mode will not lead to fainter magnitudes although in a shorter exposure time. A typical integration time for which the multiplicative errors equal the additive noise can be expressed as:

$$T_{LS}^{Sat} = \frac{1}{\phi_S (\epsilon + \omega)^2} \quad (7)$$

It strongly depends on the characteristics of the spectrograph and as an illustration, we evaluate the different limitations that will happen on two of the faint object spectrographs presently in use at ESO. In Table 1, we summarize the main characteristics: EFOSC mounted on the ESO 3.6m telescope and EMMI on the 3.5m NTT. There are two major differences between these two instruments: the CCD type (RCA thinned CCD for EFOSC, a thick low readout noise Thomson CCD for EMMI) and the spatial scale (spectral element on EMMI is reduced by a factor 2.4 compared with EFOSC). Comparison is made in two wavelength ranges where the sky spectrum behaves very differently, near $\lambda \simeq 5500 \text{\AA}$ in the sky continuum and near $\lambda \simeq 8000 \text{\AA}$ where the sky spectrum shows strong and wide emission bands

2.3. A “Va-et-Vient” mode for faint object spectroscopy

We propose a new observing mode that will minimize all the residual multiplicative errors. The main idea is to integrate the object and the sky reference alternatively on the same slit part and the same pixels in a differential mode with individual exposures short enough to avoid the introduction of errors due to the temporal sky fluctuations. Whatever the elementary exposure time, we can be still photon-noise limited, provided we read the CCD only at the end of a series of integrations. To do that, between each individual exposure, charges are transferred, without CCD readout, up or down along the chip columns synchronously with a shift of the telescope, so

that the object and the reference sky are alternatively integrated on the same pixels through the same optical path but stored in two distinct zones of the CCD. The principle of the technique is displayed in more details in Figure 1 where the four first steps of the process (2 “Va-et-Vient”) are shown. From the top to the bottom of the figure one can see:

- first step: elementary integration on the object ($t_0 \rightarrow t_1$).
- second step: the shutter is closed, the charges are transferred and the telescope is moved ($t_1 \rightarrow t'_1$). When the shutter re-opens, the integration is done on the reference sky. The object signal is stored on a blind zone of the chip ($t'_1 \rightarrow t_2$).
- third step: the shutter is closed, the charges are transferred in the opposite direction and the telescope is moved back to its initial position. When the shutter reopens, a new integration begins on the object. Integration is performed on the same physical pixels as during the first step, and the charges are added in the pixels of the object ($t_2 \rightarrow t_3$).
- fourth step: same as the second step ($t_3 \rightarrow t'_3 \rightarrow t_4$).

After n “Va-et-Vient”, the CCD is read and two strips of spectra appear on the final image, one corresponding to the object and the other to the reference sky. In what follows, the dead time between each shift, which is a few seconds on a telescope, is neglected for simplicity. The sky is first removed pixel by pixel without any smoothing. The error on the flat-field correction applies only to the object signal and the sampling residual noise $\omega\phi_S$ is set to zero. The sky fluctuations are minimized as the total exposure is segmented into individual time intervals, which can be suited to the characteristic time scale of the continuum and sky lines fluctuations (*i.e.* a few minutes). These fluctuations have different variation laws during the night or from one night to the next.

The idea of chopping spectroscopy was already used during the 1970’s with photon counting system detectors having no readout noise (Bocksenberg, 1975, Shekhtman and Hiltner, 1976). The difference with a CCD is that one cannot read the detector after each short telescope shift, so we propose to move the charges on the detector without reading it. An equivalent method has been successfully implemented in an imaging polarimeter (McLean, 1981).

With a single slitlet, half of the total telescope time would be spent integrating the reference sky and to save telescope time, we propose to use two slitlets as shown in Figure 2. In that case, the object is integrated during the total telescope time as it is positioned during half of the time on one slit and the rest of the time on the other. The charge shift must be

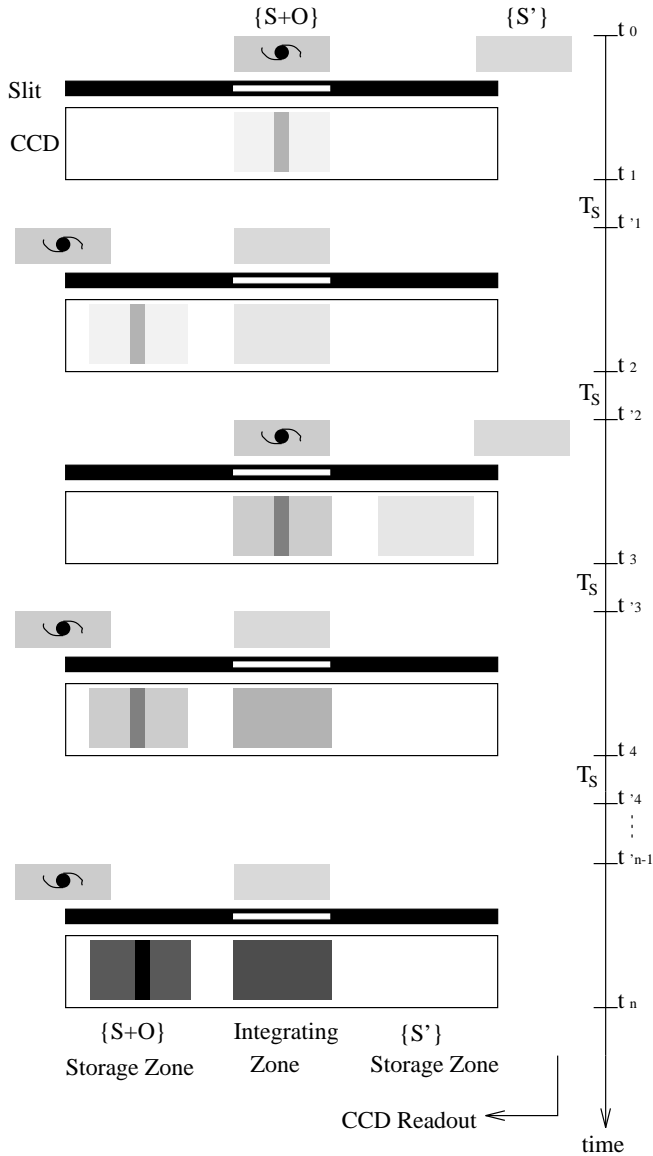


Fig. 1. Configuration of the CCD and the telescope during a “Va-et-Vient” spectroscopic exposure. Relative positions of the telescope pointed on the object $\{O + S\}$ and on the adjacent sky $\{S'\}$ appear on the figure as the corresponding charges are moved on the CCD. The projection of the slit on the CCD determines the physical integration zones. In order to avoid any mixing of the data, a slitlet is needed to mask the light from the sky in the storage zones. The time Δt between t'_i and t_{i+1} is the elementary exposure time (1 shift or 1/2 “Va-et-Vient”). T_S represents the time interval during which the shutter is closed, while the telescope is moved and the charges are shifted. Only half of the telescope time is used to integrate the object spectrum.

exactly equivalent to the telescope shift and three bands are present on the CCD at the end of the exposure. The object is on the central band and the reference sky is split over the two adjacent zones, which are both integrated half the total exposure time on pixels which receive enough flux to be in a linear regime better than few thousands whereas we work at the hundredth scale. In any case it could be possible to operate some calibrations. The main concerns for the definition of the

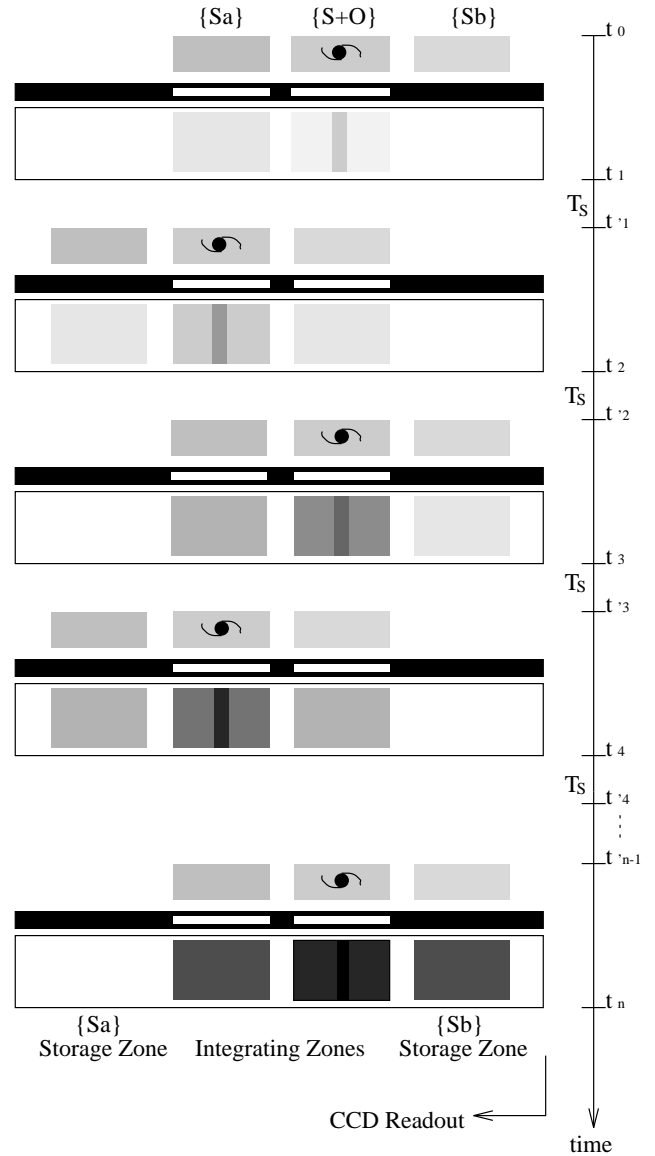


Fig. 2. Same as figure 1 in the case of two slitlets. In this case, the telescope is moved so that the object is located on one slitlet and in the other one. After the CCD readout, 3 spectroscopic bands appear on the image, containing respectively the object $\{S + O\}$ and the reference sky split in $\{S_a\}$ and $\{S_b\}$. The telescope time is fully used to integrate the object spectrum.

geometry of the two slits mode are the selection of empty sky areas on both sides of the object and the telescope pointing and shifting accuracies which must be better than a fraction of a pixel. But an extra advantage of this double slit setting is a better correction of temporal sky fluctuations which are reduced to second order values. Note that this figurative example is not optimized to save space on the CCD, slits should not be larger than the object. Moreover a single continuous slit would be sufficient for this full time object integrating mode as no gap is needed between the strips. Finally, we note that other configurations are also possible with four strips (a double one slit mode).

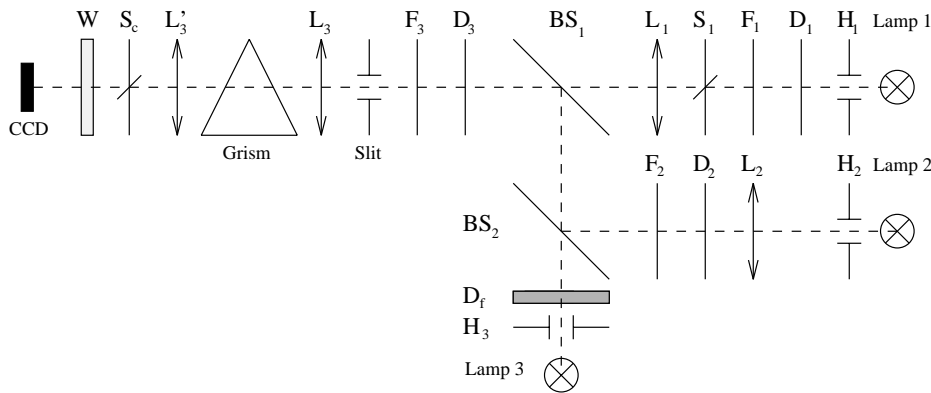


Fig. 3. Schematic diagram of the optical setting of the laboratory experiment to test the “Va-et-Vient” spectroscopic mode (see details in the text).

In principle, the few charge transfers involved should not add any additional sources of noise, so after the pixel by pixel sky subtraction ($u = 1$), neglecting the second order terms on ϕ_S , the S/N on a spectral element is now:

$$\left(\frac{S}{N}\right)_{VV} = \frac{\phi_O T}{\sqrt{2\phi_S T + 2\sigma_{CCD}^2 + \beta\phi_S T + \epsilon\phi_O T}} \quad (8)$$

where $\epsilon\phi_O T$ is the error on the flat-field correction which this time applies only to the object signal and $\beta\phi_S T$ is the error on the temporal sky variations, where β is a function of the temporal variation of the sky brightness. As in the case of the long slit spectroscopy the upper limit of the S/N is given by:

$$\left(\frac{S}{N}\right)_{VV}^{lim} = \frac{\alpha}{\beta + \alpha\epsilon} \quad (9)$$

where $\alpha = \phi_O/\phi_S$ is the object to sky brightness ratio.

The integration time for which the S/N deviates from the photon-noise regime is:

$$T_{VV}^{Sat} = \frac{2}{\phi_S(\beta + \alpha\epsilon)^2} \quad (10)$$

This value can be much higher than the previous one in the long slit mode, provided the object is very faint ($\alpha \ll 1$) and the temporal sky fluctuations are reduced enough. For example, if we use the observing conditions of EFOSC in the sky continuum, we find a value of 55 hours for the saturation time in the “Va-et-Vient” mode. This value will be reduced by a factor of 5 on a VLT with an equivalent spectrograph (same spectral element). Consequently, the “Va-et-Vient” mode can be considered as a mode that always works in a photon noise regime.

2.4. Factor of merit of “Va-et-Vient” spectroscopy

Neglecting the readout noise, we define the gain of the “Va-et-Vient” mode by the ratio between the S/N obtained in the two modes, for the same integration time and for an object fainter than the sky background:

$$G_{VV} = \frac{1 + (\epsilon + \omega)\sqrt{\phi_S T}}{\sqrt{2} + (\beta + \epsilon\alpha)\sqrt{\phi_S T}} \quad (11)$$

As expected, the behaviour of this ratio strongly depends on the factor $\sqrt{\phi_S T}$. At low values, G_{VV} tends to the value $1/\sqrt{2}$, in this regime, the “Va-et-Vient” mode is less efficient than long slit spectroscopy, because of the pixel-to-pixel sky subtraction procedure. On the contrary for high values, the gain in the “Va-et-Vient” tends to:

$$G_{VV}^{Sat} = \frac{\epsilon + \omega}{\alpha\epsilon + \beta} \quad (12)$$

a value that can greatly exceed 1, as the coefficient ω strongly dominates ϵ at low resolution near sky lines and because the parameter β can be minimized as desired as the elementary exposure time is lowered. The gain will be even higher as soon as the object-to-sky brightness ratio α is lower.

3. The “Va-et-Vient” laboratory simulation

We have shown theoretically that the “Va-et-Vient” technique is almost free of multiplicative noises, provided the charge shifts do not introduce any new sources of noise. This is why, before implementing the technique on a telescope, we carried out a laboratory experiment to fully test it and to measure the expected performance.

3.1. General description of the bench

A schematic diagram of the one slitlet experiment is displayed in Figure 3. The spectrograph is simply made with a collimator and a camera with a magnification factor of 2. Focal ratios are chosen so that the dispersion given by the grism inserted in the parallel beam is about $25 \text{ \AA}/\text{pixel}$ and the slit width corresponds to 4 pixels on the CCD. Three light sources are used to simulate respectively the sky continuum, the sky emission lines and the “galaxy”. The spectral energy distributions are not realistic but levels can be adjusted to actual astronomical spectra CCD counts. The galaxy is simulated by a pinhole ($15 \mu\text{m}$ diameter, H_1) illuminated by a halogen lamp (Lamp 1) filtered by a blue filter F_1 (Kodak filter 85B) to introduce a given spectral energy distribution in the galaxy. The hole is focused on the slit through the lens L_1 with a physical size of

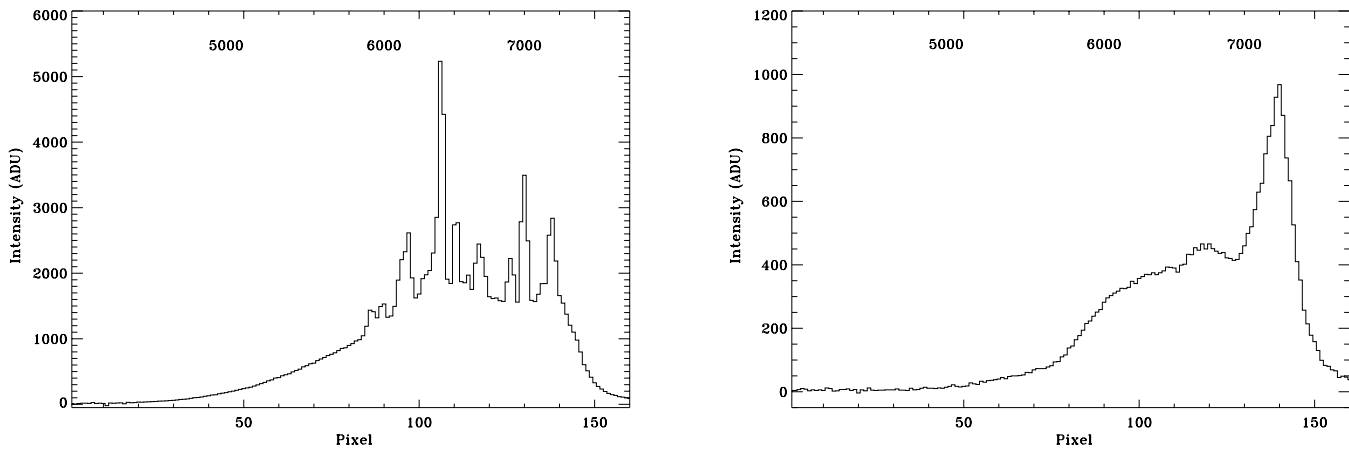


Fig. 4. Example of the spectra used in the simulation. Figure 4a represents the sky spectrum, with both a continuum and emission lines. Figure 4b represents the “galaxy” spectrum. Both spectra are obtained with a 120s exposure, and the object-to-sky ratio is about 20 % in the continuum. An approximate wavelength scale is given in Å above the spectra.

40 μm , similar to the slit width. The sky beam is a combination of two sources of light through a beam splitter BS_2 : the continuum is given by a halogen lamp (Lamp 3) illuminating a 10mm diameter hole (H_3). To improve the spatial uniformity, a scattering glass D_f is located on the beam. The emission lines are given by a neon lamp (Lamp 2). The sky lines and object beam levels can be attenuated with respect to the sky continuum through a set of densities (D_1 and D_2). The three beams are finally combined through the beam splitters BS_1 and BS_2 . An Athervex filter (F_3) cuts the strong far-red flux to avoid the fringing effects redward 7500 Å. Resulting spectra are shown in Figure 4 for the sky and the galaxy.

The shifts of the telescope between the galaxy and the sky reference are simulated by a shutter located on the object beam (S_1). When it is closed the integration is performed on the reference sky and when it is opened the object and the sky are integrated together. The CCD does not move and the same sky is integrated on each exposure, without any spatial sky fluctuations. Random temporal fluctuations have been added by introducing an interference filter in front of the sky lines beam (F_2 , DA589 filter). Tilting this filter from 0 to 30 degrees modifies the transmission depending on the wavelength so that the fluctuations are different from one line to the other. The stability of the halogen lamps has been tested as being better than 1%. Finally fluxes have been adjusted to simulate in a 10 second exposure, data obtained in one hour on a 4 meter class telescope.

3.2. Implementation of the “Va-et-Vient” mode on the CCD

We used a thinned THOMSON 512×512 CCD (TH7895, pixel size of 19 μm) four phases clocked so that the physical structure is designed to enable charge transfers in both directions along columns, what is a necessary condition to implement a “Va-et-Vient” mode. Two phases or virtual phase CCDs are not suited to this mode because of their ionic implantation which fixes the transfer direction (McLean, 1989). The readout noise of the CCD is smaller than 15 electrons with a gain of 2 electrons per analogic-to-digital unit (ADU). We used the new controller developed and designed by ESO (ESO, 1992). The implementation of the “Va-et-Vient” mode on this con-

troller consists in minor modifications of the software to clock the phases correctly. Only parameters like the number of exposures, the elementary exposure time and the number of shift lines must be added. The shutter S_1 is controlled after each clocking sequence for closing or opening.

3.3. Measurements of the Charge Transfer Efficiency and the “Va-et-Vient” noise

The first step of the experiment was to check the readout noise in the “Va-et-vient” mode compared to a normal bias frame. An image was produced by reading the CCD after a large number of shifts (typically 60 “Va-et-Vient” of 100 lines) and a standard bias frame was subtracted. The variance of the signal on the resulting image is given by:

$$V = 2\sigma_{CCD}^2 + \sigma_{VV}^2 \quad (13)$$

where σ_{VV}^2 is the variance due to the “Va-et-Vient” process. σ_{VV} was found smaller than 1 electron RMS, confirming that this noise is negligible. However it is important to note that this result holds only if the shift of charges is implemented on CCD rows that are “free” of charge traps (Blouke et al., 1987). Note that a method of multiple back-and-forth shifts of charges, called pocket pumping technique, can be used to characterize small traps on the CCD at low light level (Janesick et al., 1992).

Furthermore, as charges are transferred many times along columns, the Modulation Transfer Function (MTF) can be degraded by transfer inefficiency. A large number of shifts (1000) of many lines (100) was done on a sharp profile which was then analyzed. In this case, 200,000 charge transfers were made and we can evaluate the transfer inefficiency along the columns by modelling the resulting profile compared to the initial one. We found a value of $1 - 3.10^{-6}$ for the Charge Transfer Efficiency (CTE), typical of modern Thomson CCDs (Mellier et al., 1985). This method of evaluation of the CTE could be a complementary test of the usual method (Janesick et al., 1987). When the “Va-et-vient” mode is used in real conditions on a telescope, the number of charge transfers is kept much smaller so that we can neglect the small degradation due to the enlargement of the profile in both directions along the columns.

4. Data processing and analysis

4.1. Data reduction

The experimental data were reduced with an upgraded version of our own software developed for faint object spectroscopy and multi-object spectroscopy (Soucail et al., 1987). The main steps are: bias subtraction, flat-fielding, sky subtraction and wavelength calibration. In the present case flux calibration is not introduced.

For the long slit spectra, the reference sky is averaged over 60 lines ($u \simeq 0$) and subtracted with an optimal algorithm similar to the one proposed by Horne (1986). The object is added over 5 lines, and the data reduction produces a final one-dimensional spectrum of the object. For the “Va-et-Vient” data, a slightly different data reduction procedure is needed: after the bias subtraction, the sky subtraction is performed through a pixel by pixel operation between the two strips of the “Va-et-Vient” image. This 2D image is then flat-fielded and the optimization algorithm is applied to extract the object spectrum from the 5 lines that the object is spread over. Globally the two sets of data are recorded and reduced in a similar way, except for the sky subtraction, so they are affected by the same sources of noise.

4.2. Analysis of the experimental S/N

In a first experiment, we computed the S/N in the two modes versus the exposure time, to check the behaviour proposed in equations (5) and (8). The S/N is not easy to measure on an individual spectral element as it would imply reducing a large number of identical data, so like on astrophysical data, we measure a mean $\langle S/N \rangle$ on several spectral elements. The wavelength domain used for the calculation extends from 5800 Å to 7200 Å where the continuum is rather flat and the S/N is measured on a spectrum which results from the subtraction of a very high S/N spectrum normalized to the observed one, obtained by averaging a large number of spectra of the object lamp alone (Fig. 4b). The minimum exposure time is about 2 seconds to avoid problems due to the rising time of the shutter. To obtain the equivalent of a very long exposure time, or a high flux level in the strong sky lines, without saturating the CCD, we co-added many “Va-et-Vient” exposures before any step in the data reduction.

Results of one experimental set of data are shown in log-log scale in Figure 5 in the case of the complete sky spectrum and in Figure 6 without the sky emission lines, in order to illustrate the effects of the undersampling residuals. As expected, Figure 5 shows that the S/N varies as the sky photon noise regime with a slope of 1/2 in the two modes at low flux levels. At a higher level the S/N in the long slit mode saturates while the S/N in the “Va-et-Vient” mode does not show any departure from the photon noise regime, showing that multiplicative noises have been considerably attenuated. On a telescope, this behaviour could be slightly different because of the temporal sky fluctuations and some extra sources of noise like cosmic-ray events on the CCD in the case of long exposures.

Since this experiment confirms our analysis, we can estimate the theoretical gain in the “Va-et-Vient” mode in terms of limiting magnitudes. Using typical values of the different parameters and an object to sky ratio of $\alpha = 0.1$, we find a gain G_{VV} of 1.6 or 0.6 magnitudes in the continuum and a gain of 10, or 2.5 magnitudes in the emission lines where the sampling

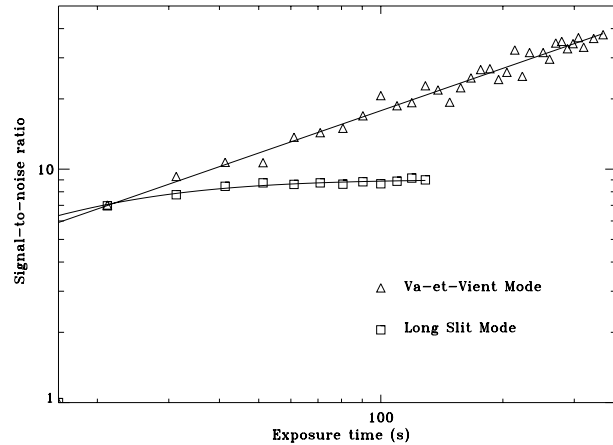


Fig. 5. S/N versus integration time for the long slit and the “Va-et-Vient” modes acquired in the same operating conditions and reduced with the same calibration data.

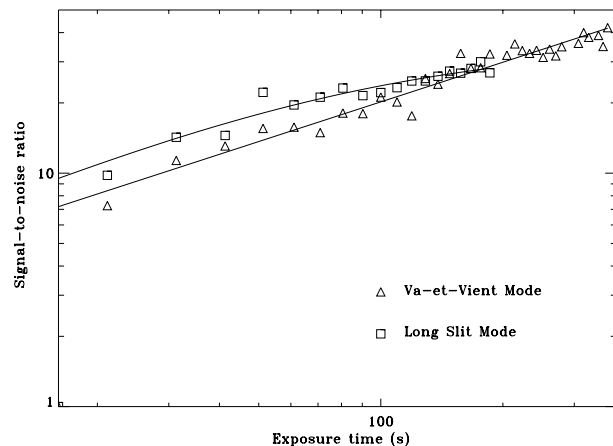


Fig. 6. Same as Figure 5, but without sky emission lines. Only the residuals in the flat-field correction degrade the S/N . The gain of the factor $\sqrt{2}$ in the long slit mode at low S/N is clearly visible.

errors dominate. It will be important to measure the maximum gain of the “Va-et-Vient” spectroscopy on real data obtained on a telescope, although this will need a dedicated observing run.

To disentangle sky line residuals from flat-field residuals in the long slit mode, we carried out the same experiment on a sky with a pure continuum (the sky lines being switched off, i.e. $\omega = 0$). The object-to-sky brightness ratio was about 26%. Figure 6 shows the results of this set of measurements and as expected, the “Va-et-Vient” curve is similar to the one in the previous experiment but the long slit mode is more competitive up to a higher level (about 8000 electrons). At lower levels, the gain factor $1/\sqrt{2}$ is in favor of the long slit mode, as expected. These results confirm that at very low dispersion, the residuals due to the subtraction of the sky lines are the dominant source of noise.

Figure 7 is an illustration of typical residual results after the sky subtraction between the restored object and the reference spectrum. The sampling noise appears clearly on the long slit residuals (Fig. 7a) as the glitches positions correspond exactly

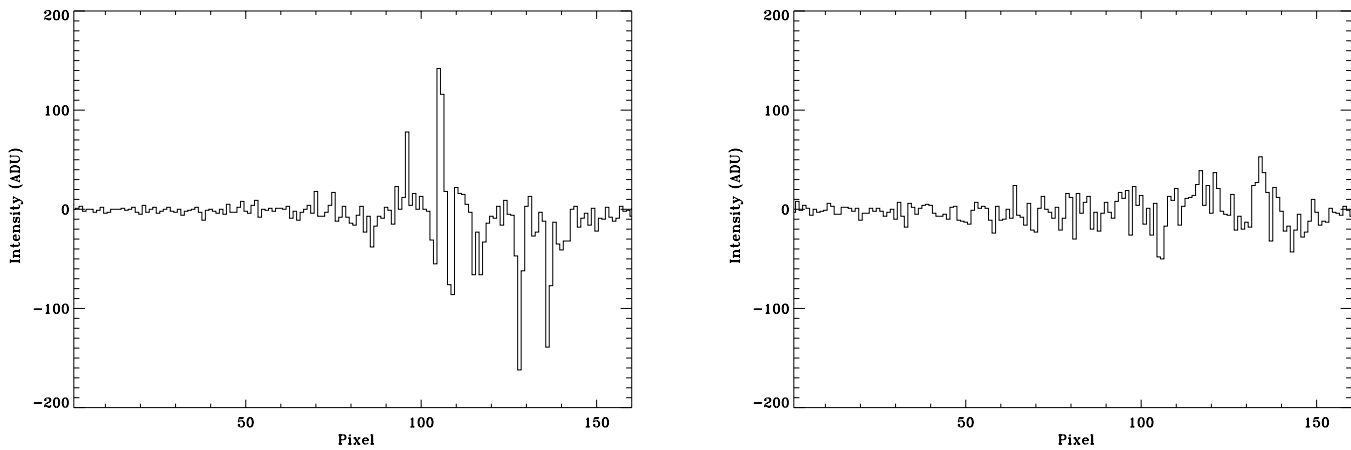


Fig. 7. Residuals of the sky subtraction in the two spectroscopic modes. A reference spectrum of the object is produced with the galaxy alone and the same exposure time. Figure 7a represents the difference between the object and the reference spectrum in the long slit mode. Figure 7b is the same for the “Va-et-Vient” mode.

to the strong sky lines (Fig. 4a). The two regimes described above appear on these curves: from pixel 1 to pixel 80, the noise in the “Va-et-Vient” mode is $\sqrt{2}$ times greater than in the long slit mode (readout noise plus photon noise) and from pixel 80 to pixel 140, the sampling noise is dominant in the long slit spectrum.

The efficiency of the “Va-et-Vient” mode in eliminating sampling noise introduced by a slit misalignment has also been tested. We rotated the slit by about 2 degrees and we checked that the S/N in the “Va-et-Vient” mode was not degraded, contrary to the long slit spectra. This consequently shows that the “Va-et-Vient” mode could work at faint levels with a curved slit or any peculiar shape. This advantage is of great interest for the spectroscopic study of faint gravitational arcs (Soucail et al., 1988) when it is necessary to integrate the flux all along a structure which presents a curved shape.

4.3. Fringing

We worked with a backside illuminated CCD which presents strong fringing effects in the far-red spectrum. For most of the tests, an athervex filter was used to cut wavelengths above 7500 Å. But we also removed the filter to check the ability of the “Va-et-Vient” mode to remove some of the fringing effects on sky limited exposures. Sky emission lines produce an interference pattern mostly in the red with a structure which depends on the wavelength of the incident light and on the thickness of the CCD. The results of these tests showed that the sky, as well as its associated fringing pattern, were correctly removed. But the fringing pattern of the object itself was still present. Like in the photometric mode, this object pattern could be attenuated through some median filtering of many similar exposures with an object located on different places on the CCD, but it requires many images (McLean, 1989) and brings back the difficulties discussed above. In any case, it is well known that removing the fringes in spectroscopic mode is always a difficult task. This is why people prefer not to work in the far-red with thinned CCDs.

5. Implementation on a telescope

To fully validate the “Va-et-Vient” spectroscopic mode, we had to test it on a telescope in real observing conditions. Thanks to S. D’Odorico and the ESO technical staff, it was possible to make a preliminary test during a few hours of an engineering run in November 1991 during a full moon period. The acquisition software of the thick 1K×1K Thomson CCD mounted on the red arm of the EMMI spectrograph of the New Technology Telescope was modified in order to observe in the “Va-et-Vient” mode. After an individual exposure, the shutter closes while the charges shift, and the exposure stops. Then one has to manually move the telescope to its other position and to press a “continue” order to the CCD.

We worked in the 2 slits mode to improve the efficiency of the telescope, as shown in Figure 2. In order to keep the exact position of the object in at least one slitlet, the guiding star was not off-centered during the even-numbers exposures, and the telescope was left tracking. We then had to bring the guiding star back in its centering box to come back to the exact original position. This procedure is valid if the elementary integration time is short so that the guiding errors and the field rotation can be reduced to a minimum, as well as the dead time between the elementary integrations. The chopping of the telescope was chosen with a period of 3 minutes, with a dead time of less than 5 seconds between each shift. We checked that through this procedure, no flux was lost on the object, by comparing a spectrum reduced after a “Va-et-Vient” exposure with a long slit exposure of the same integration time. A new test was made in January 1993 during a run of the “Toulouse gravitational arcs survey” (Fort et al., 1991). Again only 4 hours were spent testing the “Va-et-Vient” mode, as we preferred to observe in high resolution imaging, because of excellent observing conditions and seeings. The test was successful but not complete. New observations with the “Va-et-Vient” spectroscopic mode are now proposed as a back-up program during bad seeing periods when spectroscopy is scientifically more efficient than ultra-deep imaging and photometry.

6. Conclusion

We have used laboratory simulations to prove the interest of “Va-et-Vient” spectroscopy for the low resolution spectroscopy of very faint objects with very large telescopes. As an example, with a resolution of $R \sim 300$, our simulations predict that we should reach the saturation time corresponding to a S/N of 2.5 on a long slit spectrum of a faint distant galaxy with $B=24.5$ in about half an hour exposure time on a 10-meter telescope. While in a 2 hours exposure time, with the “Va-et-Vient” mode which preserves the photon noise regime, the S/N could be increased by a factor of 3 or much for higher exposure times. The method also gains in efficiency with very large backside illuminated CCDs (size larger than $2K \times 2K$) free from trapping effects on the whole surface. In practice, the only limitation of the method above 7000 \AA will be the photon noise of the strong sky emission lines.

“Va-et-Vient” spectroscopy seems well suited to the study of very faint and slightly extended objects such as distant galaxies. Indeed, one immediate application would be to obtain the spectra of faint gravitational arcs which are known to be distant galaxies magnified by cluster gravitational lensing. Because “Va-et-Vient” spectroscopy remains efficient even with curved slits of any irregular shape, this new observing mode is well adapted for the observational program of a spectroscopic survey of gravitational arcs. More generally, the implementation of the “Va-et-Vient” mode on multislit spectrographs could be possible with a dedicated software for the selection of objects. As sky subtraction is made pixel-to-pixel, the slits have not to be longer than the object extension and the space used per object to store charges on the CCD is approximately three times the slit size. The main requirement is that two nearby symmetrical sky references must be found at the same distance of all objects. For empty fields, the simultaneous observation of about 15 extremely faint objects within a field of view of 7×7 arcmin. square can be expected. With long exposure times on very large telescopes, the deepest spectroscopic survey could be extended at least to one magnitude fainter than those presently done at the same S/N .

In conclusion, the faint object “Va-et-Vient” spectroscopic mode seems to be a potentially powerful technique to take full advantage of the large light collecting area of the new very large telescopes. It is difficult to completely evaluate the method with 3.5 meter class telescopes because their light collecting area is not large enough to rapidly reach the S/N saturation level with regular exposure times. Therefore it would be interesting to try a complete evaluation of the mode on the Keck Telescope since a new spectroscopic window on the distant universe would be opened.

Acknowledgements. This work was supported by the Centre National de la Recherche Scientifique and the Université Paul Sabatier. We wish to thank Sandro D’Odorico (ESO) for the 2 nights of engineering time on the NTT he allocated for testing

the “Va-et-Vient” spectroscopy and also the technical staff in Garching and La Silla who have played a role in its final implementation on the NTT. Many thanks also to Y. Mellier and G. Mathez for the fruitful discussions about the future of faint object spectroscopy on large telescopes and to M. Dantel-Fort for her help in the data reduction. We also thank S.J. Lilly, referee of this paper, for his pertinent remarks.

References

- Bocksenberg A., 1975, in “Image Processing Techniques in Astronomy”, C. de Jager and H. Nieuwenhuizen eds., Reidel.
- Blouke M.M., Yang F.H., Heidtmann D.L., Janesick J.R., 1988, in “Instrumentation for Ground-Based Optical Astronomy: Present and Future”, L.B. Robinson Ed., Springer-Verlag, p. 462
- Colless M., Ellis R.S., Taylor K., Hook R.N., 1990, MNRAS 244, 408
- Colless M., Ellis R.S., Broadhurst T.J., Taylor K., Peterson B.A., 1993, MNRAS 261, 19
- Cowie L.L., Lilly S.J., 1989, ApJ 336, L41
- Cowie L.L., Gardner J.P., Hu E.M., Wainscoat R.J., Hodapp K.W., 1993, ApJ submitted
- ESO document VLT-PLA-ESO-13200-0230, 31st meeting of the Scientific Technical Committee, VLT Instrumentation Plan, April 16 1992
- Fort B., Le Borgne J.F., Mathez G., Mellier Y., Picat J.P., Soucail G., Pelló R., Sanahuja B., 1991, The Messenger 62, p. 11
- Horne K., 1986, PASP 98, 609
- Janesick J.R., Elliot S.T., Collins S.A., Blouke M.M. Freeman J.W., 1987, Opt. Eng. 26, 692
- Janesick J.R., Elliot S.T., ASP Conference Series, Vol. 23, 1992, Steve B. Howell, ed.
- Lilly S.J., Cowie L.L., Gardner J.P., 1991, ApJ 369, 79
- McLean I.S., Cormack W.A., Herd J.T., Aspin C., 1981, SPIE 290, 155
- McLean I.S., 1989, Electronic and Computer-Aided Astronomy, Ellis Horwood Library of Space Science and Space Technology
- Mellier Y., Cailloux M., Dupin J.P., Fort B., Lours C., Picat J.P., Tilloles P., 1985, A&A 157, 96
- Robertson J.G., 1986, PASP 98, 1220
- Sheckman S.A., Hiltner W., 1976, PASP 88, 960
- Soucail G., Mellier Y., Fort B., Picat J.P., Cailloux M., 1987, A&A 184, 361
- Soucail G., Mellier Y., Fort B., Mathez G., Cailloux M., 1988, A&A 191, L19
- Tyson A.J., 1986, J. Opt. Soc. Am. A. 3, 2131
- Tyson A.J., 1988, AJ 96, 1
- Tyson A.J., 1990, J. Opt. Soc. Am. A. 7, 1231

This article was processed by the author using Springer-Verlag \TeX A&A macro package 1991.